PROCEEDINGS A

rspa.royalsocietypublishing.org

Research

Cite this article: Müller R, Rode C, Aminiaghdam S, Vielemeyer J, Blickhan R. 2017 Force direction patterns promote whole body stability even in hip-flexed walking, but not upper body stability in human upright walking. *Proc. R. Soc. A* **473**: 20170404. http://dx.doi.org/10.1098/rspa.2017.0404

Received: 7 June 2017
Accepted: 12 October 2017

Subject Areas:
biomechanics

Keywords:
bipedal walking, stability, upper body, virtual pivot point

Author for correspondence:
Roy Müller
e-mail: roy.mueller@uni-jena.de

†These authors contributed equally to this study.

THE ROYAL SOCIETY PUBLISHING

Force direction patterns promote whole body stability even in hip-flexed walking, but not upper body stability in human upright walking

Roy Müller[1,2,†], Christian Rode[1,†], Soran Aminiaghdam[1], Johanna Vielemeyer[1] and Reinhard Blickhan[1]

[1]Motionscience, Institute of Sport Sciences, Friedrich Schiller University Jena, Seidelstraße 20, 07740 Jena, Germany
[2]Department of Neurology/Department of Orthopaedic Surgery, Klinikum Bayreuth GmbH, Hohe Warte 8, 95445 Bayreuth, Germany

RM, 0000-0002-4688-1515

Directing the ground reaction forces to a focal point above the centre of mass of the whole body promotes whole body stability in human and animal gaits similar to a physical pendulum. Here we show that this is the case in human hip-flexed walking as well. For all upper body orientations (upright, 25°, 50°, maximum), the focal point was well above the centre of mass of the whole body, suggesting its general relevance for walking. Deviations of the forces' lines of action from the focal point increased with upper body inclination from 25 to 43 mm root mean square deviation (RMSD). With respect to the upper body in upright gait, the resulting force also passed near a focal point (17 mm RMSD between the net forces' lines of action and focal point), but this point was 18 cm below its centre of mass. While this behaviour mimics an unstable inverted pendulum, it leads to resulting torques of alternating sign in accordance with periodic upper body motion and probably provides for low metabolic cost of upright gait by keeping hip torques small. Stabilization of the upper body is a consequence of other mechanisms, e.g. hip reflexes or muscle preflexes.

1. Introduction

Habitual bipedalism has evolved multiple times in several different animal orders. Two highly successful

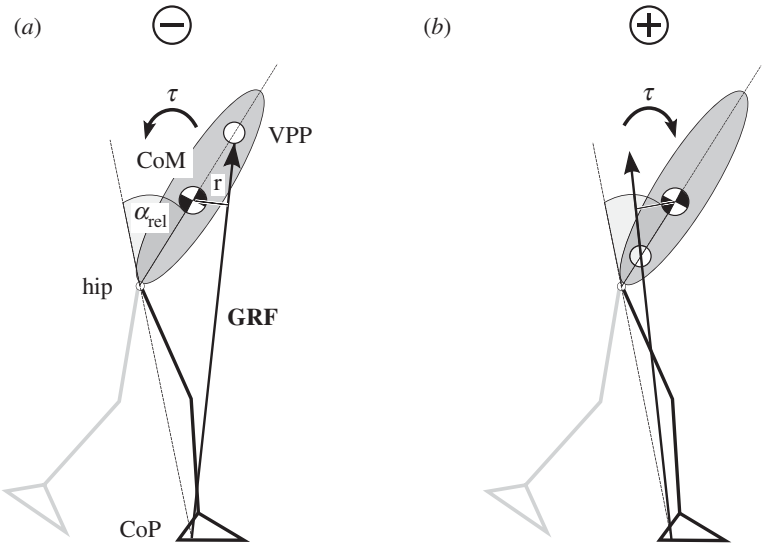

Figure 1. Effect of virtual pivot point (VPP) height. The trunk represents the mass of the whole body; the legs are massless. If the VPP is above the centre of mass (CoM), then the ground reaction force (**GRF**) results in torque $\tau = \mathrm{r}\cdot\mathrm{GRF}$ (r, perpendicular distance between the line of action of the **GRF** and the CoM; GRF, magnitude of **GRF**) that counteracts the rotation of the trunk away from the hip–centre of pressure (CoP) axis (*a*, negative feedback). If the VPP is below the CoM, then the **GRF** enhances rotation away from the hip–CoP axis (*b*, positive feedback). Notably, the direction of the feedback is independent from the magnitude of the **GRF**. Note that the angle relevant for the feedback, α_{rel}, is measured between the trunk and the hip–CoP axis (dotted line).

species which have individually evolved bipedalism are birds and, with significantly shorter bipedal history, early hominids [1,2]. In contrast to quadrupeds, one central problem in understanding the success of bipedal gait is how the whole body can be stabilized when only two legs support it. Moreover, bipedal species must balance the heavy upper body (whole body without legs).

Using simplified models of the locomotion system, researchers have investigated the neural, mechanical and neuro-mechanical mechanisms that may have facilitated the evolution of bipedalism [3,4]. The detail of the model depends on the research question. For example, the bipedal spring-mass model (a point mass supported by two massless leg springs) can be used to predict the global dynamics (ground reaction forces (GRFs) and centre of mass (CoM) movement) of both human [5,6] and avian walking [7]. Replacing the point mass with a rigid body (a trunk that comprises the whole mass of the body and possesses the mass moment of inertia; figure 1), Maus *et al*. [8] suggested that humans stabilize walking by directing the GRFs to a point above the CoM of the whole body. They termed this point the *virtual pivot point* (VPP) and speculated that its supportive function may have assisted in the transition to erect hominine walking.

More precisely, in the VPP model, a trunk-fixed VPP (i.e. the VPP rotates with the trunk) is the target variable controlling the direction of the GRFs. During stance, hip torques are adjusted in such a way that the GRFs intersect the VPP. Depending on the VPP location, this can lead to a negative or a positive feedback of the GRFs on the relative trunk angle, i.e. the angle measured between the trunk and the hip–centre of pressure (CoP) axis (figure 1). Provided the VPP is above the CoM, then hip torques tend to decrease deviations between the trunk and hip–CoP axes (figure 1*a*, negative feedback). This negative feedback stabilizes the VPP model for upright [8] and for pronograde gait [9]. If however the VPP is below the CoM, then hip torques tend to increase deviations between the trunk and hip–CoP axes (figure 1*b*, positive feedback).

Interestingly, using a bipedal spring-mass model with a trunk, it has been shown that an approximate VPP can emerge purely from mechanics by introducing hip springs [10], and an exact VPP can result from leg force feedback adjusting the stiffness of hip springs [11]. It

is however not clear whether the VPP is a target variable in the control of human walking, or whether a VPP emerges from other neural control mechanisms (e.g. reflexes) using other target variables (e.g. upper body orientation). In both cases, such control loops would work in combination with mechanics (e.g. preflexes [12]) and feed-forward control. The occurrence of a VPP in humans and other animals [8,9,13] may be due to a long process of neuro-mechanical adaptation. However, the feasibility of locomotion is not assumed to be dependent on the intersection of the GRFs in a point above the CoM [14]. Thus, it might be expected that if the body mechanics are strongly perturbed—for example, by inclining the heavy upper body forward in human walking, leading to an altered operation of the legs' extensor–flexor system [15] and a changed relation between body kinematics and kinetics [16,17]—GRFs would not pass similarly close to a VPP or might even not intersect at a point at all.

Independent of the question of cause and effect, walking simulations with the VPP model resulted in partially stable upright walking [8] and stable pronograde locomotion [9]. This means that *the model* can stabilize its posture if GRFs intersect in a body-fixed VPP. However, in upright walking, the fluctuations of the model's trunk pitch angle were opposite to the upper body angle of humans [14,18,19]. This sheds some doubt on the relevance of the VPP concept for upper body stability in human upright walking. Because of the legs' mass, the force acting on the upper body is different from the GRF. Hence, a VPP of a GRF is not sufficient to understand the angular motion of the upper body. To assess whether the upper body is stabilized like a physical pendulum (similarly to the whole body), it is necessary to test whether the lines of action of the equivalent force (replacing resulting hip force and torque) acting on the upper body pass near a focal point (FP) and whether this point is located above the centre of mass of the upper body (CoM_{UB}).

Therefore, the purpose of this study was twofold: (i) to investigate whether GRFs approximate a VPP in human walking with an atypical forward-bent upper body and compare its position and quality with regular upright walking, and (ii) to test whether the equivalent force acting on the upper body passes near a FP and to *determine* whether it is located above the CoM_{UB}.

2. Methods

Ten subjects (mean ± s.d., age: 26.0 ± 3.7 years, mass: 65.2 ± 5.7 kg, height: 169.5 ± 4.8 cm) took part in this study. All of them walked at a self-chosen constant speed along a 12 m walkway with two consecutive force plates in its centre (Kistler, Winterthur, Switzerland). The GRFs were sampled at 1000 Hz. After normal upright walking, the subjects walked with a 25° (TI25), 50° (TI50) and maximally inclined upper body (TImax; figure 2). While there was no comparison for TImax, upper body target angles in TI25 and TI50 gaits were compared visually with adjustable-height cardboard templates by a second examiner prior to performing each trial and during gait along the walkway [16]. The subjects accomplished eight trials where consecutive contacts were on individual force plates.

Reflective markers were placed on the distal head of the fifth metatarsal bone, on the lateral malleolus, epicondylus lateralis, trochanter major, posterior superior iliac spine, acromion process, lateral humeral epicondyle and distal radius on both sides of the body, as well as on the L5 and C7 processus spinosus. All trials were recorded with eight cameras (240 Hz) of a three-dimensional infrared system (MCU 1000; Qualisys, Gothenburg, Sweden) and synchronized with force data acquisition.

Kinetic and kinematic data were analysed using custom written Matlab code (The Mathworks, Inc., Natick, MA, USA). GRFs were normalized to subject body weight (BW). The raw kinematic data were filtered with a third-order low-pass Butterworth filter at a 50 Hz cut-off frequency [20]. At touchdown (GRFs exceed 0.02 BW), we calculated the upper body inclination (the angle enclosed by the line through L5 and C7, and the vertical [21]) and the positions of the CoM and CoM_{UB}. The vertical and horizontal motion of the CoM (which comprises the whole body segments) and the CoM_{UB} (which comprises the forearm with hand, the upper arm, and the trunk with head segments) were determined by the body segmental analysis method [22]. The locations of the segmental CoMs were determined from the positions of the markers that were

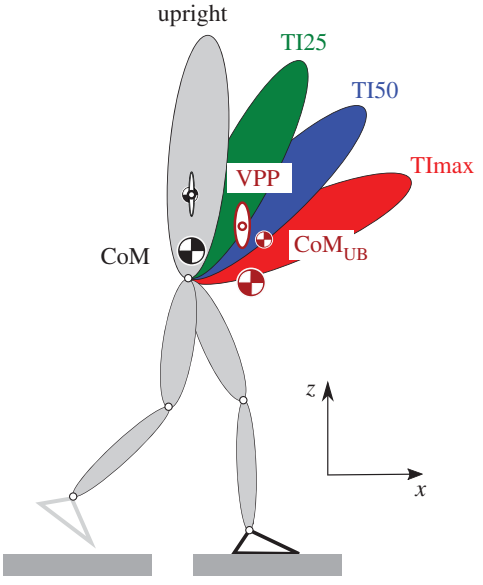

Figure 2. Experiments and associated changes in the location of the centre of mass of the whole body (CoM) and the upper body (CoM$_{UB}$), and the virtual pivot point (VPP). Subjects walked along a walkway with two integrated consecutive force plates with four different trunk inclinations (upright, black; 25° (TI25), green; 50° (TI50), blue; maximal upper body inclination (TImax), red). In human upright walking, the CoM is above the hip and below the CoM$_{UB}$, and the CoM$_{UB}$ and VPP locations coincide. In walking with an inclined upper body, the CoM and CoM$_{UB}$ shifted anteriorly and inferiorly (shown here for TImax) relative to the hip. The VPP (ellipses; main axes equal two times standard deviation) shifted in the same directions, but was less pronounced. (Online version in colour.)

placed on the body. Body mass segment fractions were based upon data from Harless [23], and segmental lengths were from data by Dempster [23]. To determine the VPP, we first subtracted the horizontal and vertical CoM coordinates from the CoP coordinates and drew the scaled GRFs into a CoM-centred coordinate frame aligned with the vertical [8,14]. The VPP location minimized the sum of the squared perpendicular distances from the VPP to the measured GRF lines of action from 0.1 to 0.9 of stance [14].

We determined the equivalent force $\mathbf{F}_e$ (replacing resulting hip torques and forces) that acts on the upper body from literature data of the single support phase of upright walking at a speed between 1.5 and 1.6 m s^{-1} (data are shown in the Results section). More specifically, $\mathbf{F_e}$ equals the resulting hip force [24], and its signed distance relative to the hip is given by dividing the resulting hip torque (the sum of the stance and swing leg torques [8]) by the force's magnitude. This yielded the location of $\mathbf{F}_e$ relative to the hip. The FP location minimized the sum of the squared perpendicular distances from the FP to the lines of action of $\mathbf{F_e}$ during the single support phase. We used four reference frames to calculate the location of the FP: the origin was at the hip or at the CoM$_{UB}$, and the frames were rotationally fixed to the upper body (using upper body rotation during single support [16] to adjust the coordinates of $\mathbf{F}_e$) and to the world, respectively. We assumed that the hip is 10 cm below the CoM throughout single support. The CoM$_{UB}$ is horizontally shifted by 1.7 cm posterior to these points at the beginning of single support (using the horizontal CoM$_{UB}$ location at touchdown and accounting for upper body backwards rotation by 1.3° in the double support phase [16]).

In order to compare kinetic and kinematic parameters, we used repeated measures ANOVAs ($p < 0.05$; SPSS®, Chicago, IL, USA) with *post hoc* analysis (Bonferroni correction) to determine statistical differences due to the posture factor (upright, TI25, TI50 and TImax). We performed a one-sample *t*-test to show that the VPP is above the CoM (separated for each upper body inclination).

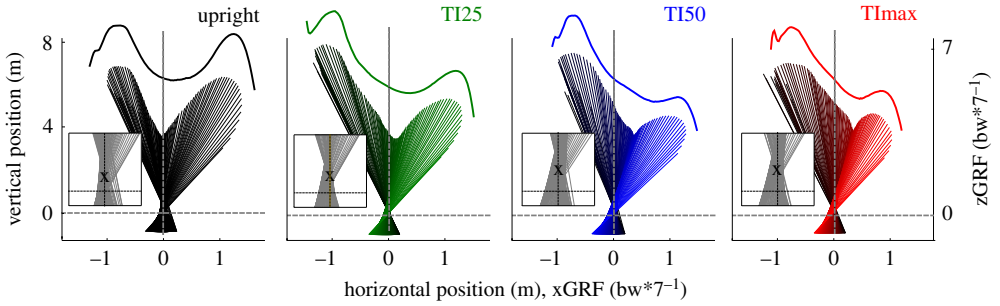

Figure 3. Virtual pivot point (VPP) in all gaits. In walking with upright and with inclined upper body configurations ground reaction forces (GRF) passed near a point (VPP, cross) relative to the centre of mass of the whole body. Lines show the GRF for typical trials of subject 9 from 0.1 (black) to 0.9 of the stance phase (colour corresponding to upper body inclination: upright, black; 25° (TI25), green; 50° (TI50), blue; maximal upper body inclination (TImax), red), originating at the centre of pressure and pointing along the line of action of the force. With increasing upper body inclination, GRFs became asymmetric, with higher forces in the first half of stance (cf. [25]). Time series of magnitude of GRFs were superimposed as coloured lines. **GRF** points upwards; its coordinates xGRF and zGRF (difference in axis values of the tip and tail of the **GRF** vectors) are plotted in 7*body weight, BW. (Online version in colour.)

Table 1. Kinetic and kinematic parameters. Mean ± standard deviation across all subjects (*N*) for the investigated kinetic and kinematic parameters: trunk inclination angle at touchdown (trunk angle at TD), walking velocity, minimum and maximum of horizontal (xGRF) and maxima of the vertical ground reaction force (zGRF), the horizontal (x) and vertical positions (z) of the centre of mass of the whole body (CoM) relative to L5, of the centre of mass of the upper body (CoM_{UB}) relative to the CoM, of the virtual pivot point (VPP) relative to the CoM, the root mean square deviation from the VPP to the measured GRF lines of action (VPP_RMSD), and the spread of GRF lines of action at the height of the VPP. Significant differences from upright walking, 25° (TI25) and 50° (TI50) inclined trunk walking are indicated with 'a', 'b', and 'c', respectively ($p < 0.05$). For statistical analysis we used repeated measures ANOVAs with *post hoc* analysis (with Bonferroni correction) and posture as the factor (upright, TI25, TI50 and TImax).

	trunk orientation			
	upright	TI25	TI50	TImax
trunk angle at TD (deg)	7.4 ± 3.1	31.9 ± 5.4[a]	47.1 ± 5.4[a,b]	72.5 ± 8.1[a,b,c]
velocity (m s^{-1})	1.49 ± 0.08	1.59 ± 0.11[a]	1.64 ± 0.14[a]	1.64 ± 0.16[a]
xGRFmin (bw)	−0.21 ± 0.04	−0.23 ± 0.05	−0.25 ± 0.06	−0.29 ± 0.08
xGRFmax (bw)	0.25 ± 0.02	0.23 ± 0.03[a]	0.20 ± 0.03[a,b]	0.19 ± 0.03[a,b]
zGRFmax1 (bw)	1.09 ± 0.11	1.18 ± 0.11	1.21 ± 0.13	1.21 ± 0.12
zGRFmax2 (bw)	0.91 ± 0.06	0.77 ± 0.08[a]	0.68 ± 0.08[a,b]	0.64 ± 0.06[a,b]
xCoM (m)	0.05 ± 0.01	0.10 ± 0.01[a]	0.13 ± 0.01[a,b]	0.16 ± 0.02[a,b,c]
zCoM (m)	−0.03 ± 0.01	−0.06 ± 0.01[a]	−0.08 ± 0.02[a,b]	−0.14 ± 0.02[a,b,c]
$xCoM_{UB}$ (m)	−0.01 ± 0.00	0.02 ± 0.01[a]	0.03 ± 0.01[a,b]	0.05 ± 0.01[a,b,c]
$zCoM_{UB}$ (m)	0.21 ± 0.01	0.20 ± 0.01[a]	0.19 ± 0.01[a,b]	0.16 ± 0.01[a,b,c]
xVPP (m)	0.00 ± 0.01	−0.01 ± 0.01	−0.02 ± 0.02[a]	−0.04 ± 0.03[a,b,c]
zVPP (m)	0.21 ± 0.07	0.25 ± 0.11	0.26 ± 0.11	0.27 ± 0.09
VPP_RMSD (mm)	24.5 ± 5.8	26.0 ± 5.4	32.1 ± 9.0[b]	42.8 ± 5.9[a,b,c]
VPP_spread (m)	0.12 ± 0.03	0.10 ± 0.02	0.11 ± 0.03[b]	0.14 ± 0.02[b]
N	10	10	10	10

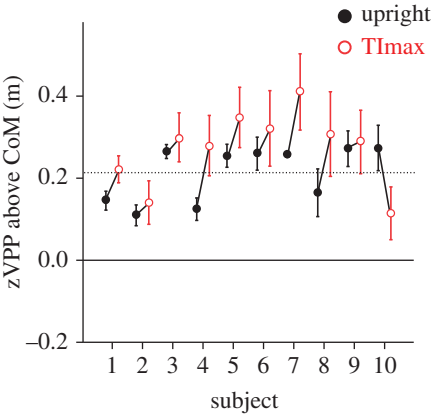

Figure 4. Variability of the virtual pivot point (VPP). For walking with upright (black) and maximal upper body inclination (red) the VPP (mean height including standard deviation (error bars)) was above the centre of mass of the whole body (CoM). Intra-subject variability increased with upper body inclination and inter-subject variability remained rather constant. The horizontal dotted line marks the vertical height of the CoM of the upper body (CoM_{UB}). Subject order is random. In subject 7 the standard deviation is below the marker size. (Online version in colour.)

Table 2. Focal point (FP) location determined using four different coordinate systems. CoM_{UB} is the centre of mass of the upper body. RMSD is the root mean square deviation of the lines of action of the equivalent force acting on the upper body from the FP. xFP and zFP are the location of the FP. FP is considerably below the CoM_{UB} in all cases (vertical distance hip–CoM_{UB} is 31 cm).

origin	alignment	RMSD (cm)	xFP (cm)	zFP (cm)
CoM_{UB}	world	1.8	−2.2	−18.1
CoM_{UB}	upper body	1.8	−1.7	−17.5
hip	world	1.7	−3.5	10.8
hip	upper body	1.7	−3.5	10.8

3. Results

When walking, humans exhibited a VPP for each upper body inclination (figure 3). However, the root mean square of the perpendicular deviation (RMSD) from the VPP to the measured GRF lines of action became larger with upper body inclination and increased from 2.5 cm for upright walking to 4.3 mm for TImax (table 1). The locations of the quantities CoM, CoM_{UB} and VPP for upright walking and walking with maximal upper body inclination are visualized in figure 2. For all upper body inclinations, the VPP was significantly above the CoM (figure 4, table 1). With increasing trunk inclination, the mean vertical distance between the CoM and VPP showed an increase from 21 cm for upright walking to 27 cm for TImax, but the population inference failed to show a difference (table 1). In the horizontal direction, VPPs shifted posteriorly relative to the CoM with upper body inclination. For maximal upper body inclination, this horizontal shift was approximately 4 cm (table 1).

Assuming that the CoM is 0.1 m above the hip, the CoM_{UB} is 0.31 m above the hip (table 1). For upright walking, the FP estimate from literature data was 11 cm above the hip (for hip-centred coordinate systems) and 18 cm below the CoM_{UB} (for CoM_{UB}-centred coordinate systems). The horizontal shift was 3.5 cm posterior to the hip for the hip-centred coordinate system and about 2 cm posterior to the CoM_{UB} for the CoM_{UB}-centred frame (table 2, figure 5). The RMSD of the equivalent force's lines of action from the FP was 1.7 and 1.8 cm for hip-centred and CoM_{UB}-centred coordinate systems, respectively (table 2). The small upper body rotation (amplitude of 1.5° during single support; figure 5*b*) had little effect on the FP location (table 2).

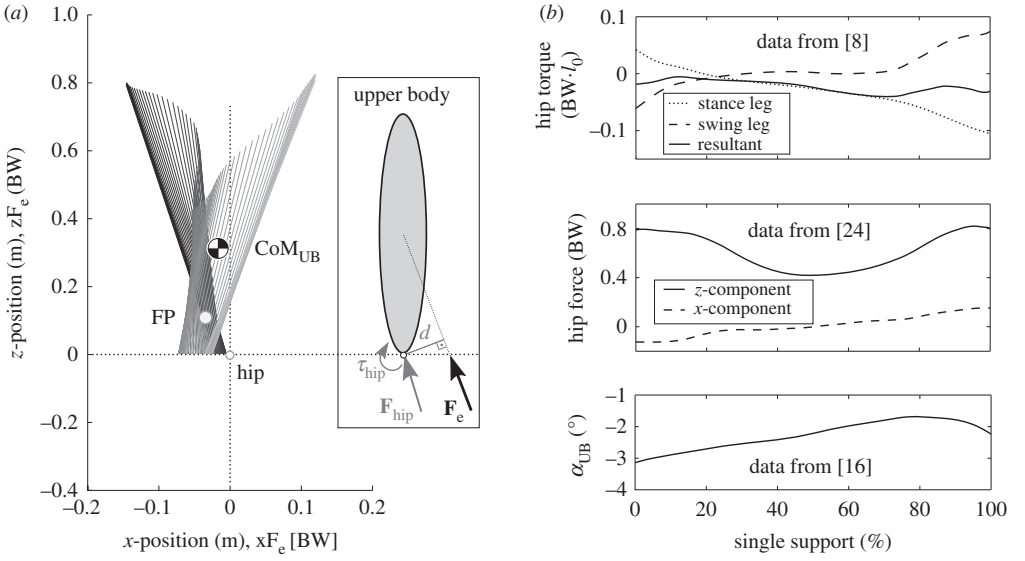

Figure 5. Pattern of the equivalent force acting on the upper body. (*a*) An equivalent force, $\mathbf{F}_e$, can replace hip force and torque acting on the upper body. Ensemble averaged resulting hip torques from [26] divided by the magnitude of hip force from [24] during the single support phase yielded the signed distance d of $\mathbf{F}_e$ from the hip (inset). Here, $\mathbf{F}_e$ is plotted into a hip-centred coordinate system rotationally fixed to the world. $\mathbf{F}_e$ points upwards; its coordinates xF_e and zF_e (difference in axis values of the tip and tail of $\mathbf{F}_e$ vectors) are plotted in body weight, BW. The focal point (FP) was located 10.8 cm above and 3.5 cm posteriorly to the hip. Upper body angular movement is small, about 1.5° during single support, corresponding to about 1 cm displacement of the centre of mass of the upper body (CoM_{UB}) relative to the hip. For comparison, the CoM_{UB} location at the beginning of single support is shown. Results are insensitive (cf. table 2) to the chosen reference frame (origin hip or CoM_{UB}) and alignment (rotationally fixed to upper body or world). (*b*) Literature data used for the determination of the FP. Hip torques (positive for extension) of stance and swing leg in BW multiplied by leg length in upright stance, l_0 (l_0 was assumed to be 0.9 m) from [8], the resulting hip force components in BW from [24], and angular movement of the upper body (α_{UB}) from [16]. α_{UB} is positive for forward rotation and zero for vertical orientation. Single support corresponds to the interval from 0.1 to 0.5 of the gait cycle [16].

4. Discussion

Our results show that, regardless of sagittal upper body orientation, GRFs pass near a VPP in human walking. However, with an increase in upper body inclination, deviations of the GRF vectors from the VPP became larger and the VPP shifted posteriorly relative to the CoM. In contrast to the whole body, the upper body seems not to be stabilized like a physical pendulum in upright walking.

(a) The virtual pivot point is above the centre of mass for all imposed trunk orientations

In human walking, for all different upper body inclinations the VPP was significantly above the CoM (figure 4, table 1). Thus it is theoretically possible that directing GRFs to the VPP is used to regulate the angular momentum of the whole body [8,9,14]. Because of this GRF pattern the angular momentum of the whole body oscillates about zero with the step frequency [18,27,28]. GRFs pointing towards the VPP generate forward angular momentum from midstance to touchdown of the contralateral leg and thus prepare for pivoting over the foot in the single support phase of the following step. Subsequent to the double support phase (which is related to load transfer), the accumulated forward momentum can be used to elevate the CoM.

This benefit of directing the force to a point above the CoM may pertain only to the walking gait due to the presence of inverted pendulum mechanics. However, a VPP has been shown experimentally to occur in other species and in other gaits as well [8,9,13], e.g. in running (where

bouncing dynamics dominate, e.g. [29]). A more general benefit of directing the GRF to a point above the CoM is that this decreases the horizontal acceleration and deceleration compared with GRFs acting along the leg axis [8], which may contribute to locomotion comfort and safety (reducing the risk of slipping).

(b) Is the virtual pivot point a target variable of control?

Understanding whether a VPP emerges from controlling target variables such as upper body orientation or by using a VPP itself as a target variable of control could be of biomechanical importance (e.g. in the control of robots or assistive devices). In human gait models, it has been shown that a VPP can arise from mechanics using hip springs [10], regulation of hip stiffness depending on the GRF [11], or from body dynamics, habitual foot rollover and hip–knee coordination [30]. Assuming an emergent VPP, which might result from tuning of feed-forward signals and control mechanisms like reflexes, more deviations of the GRFs from a VPP might be expected if human gait is challenged by experimentally prescribed, unusual upper body orientations. In accordance with this consideration, the RMSD of the GRF vectors with respect to the VPP increased significantly for TI50 and TImax (table 1). In TImax, the VPP height was up to 1.8-fold that of upright gait.

Basic features of the observed horizontal VPP shift with trunk inclination can be explained with body mechanics. For maximal upper body inclination, the CoM shifted approximately 11 cm relative to L5 anteriorly. While it might be expected that GRFs would be centred about the CoM in a trunk-flexed gait as in an upright gait, the VPP shifted up to approximately 4 cm posteriorly relative to the CoM in TImax (table 1). While the ankle torque remains nearly unchanged, the anterior CoM shift induced by upper body inclination corresponds to larger hip extension torques and less flexion torques [26], leading to a within-step asymmetry of GRFs (figure 3; see also [16]), with higher forces from touchdown to midstance than from midstance to toe-off. Under such circumstances, smaller and larger lever arms of the GRFs with respect to the CoM, respectively, are required to balance total angular momentum. This can explain the posterior shift of the VPP relative to the CoM. For different imposed upper body angles, the location of the VPP changes relative to the CoM (figure 2).

With increasing upper body inclination VPP height increases with respect to the CoM, but decreases relative to the ground (figure 2). The vertical distance between the CoM and VPP increased from 21 cm on average for upright walking to 27 cm on average for TImax, but the population inference failed to show a difference (table 1, figure 2). Moreover, the vertical position of the VPP seems to decrease with walking speed (see [8,14] and our results). Looking at the detailed data (figure 4), the subjects' mean VPP height was located 10–30 cm above the CoM in upright walking at a self-selected speed. This is in approximate agreement with the results observed during upright walking on a treadmill where the VPP was located 5–70 cm above the CoM (at speeds of 0.8–1.7 m s^{-1} [8]). It is not easily conceivable how a changing geometric, body-fixed VPP location may be represented in the central nervous system and how GRFs could be directed towards this point throughout the stance phase in each condition. In conclusion, in our view these are reasons against assuming that the VPP is a target variable of control; rather, we believe that it is the outcome of other regulatory mechanisms.

A VPP is not unique to human walking. Similar observations have been made of other animals, including dogs walking on a treadmill, chickens walking and running over even ground, and quails walking, running and ground running [8,9,13]. The idea that the VPP is an emergent property of other regulatory mechanisms does not indicate that its existence and location have no relevance for locomotion.

(c) The focal point of net leg forces is below the centre of mass of the upper body

Using ensemble-averaged resulting hip torques [26] and forces [24] of upright walking during the single support phase from the literature, we found that the equivalent force acting on the

upper body passed near an FP during the single support phase, but that the FP height (13 cm) was considerably lower than the CoM_{UB} height (31 cm; figure 5). This means that the upper body is certainly not stabilized like a physical pendulum, as suggested by the VPP model (which comprises the whole mass of the body in a rigid trunk).

The hip torques of the swing and stance legs counteract each other (figure 5*b*). Hence, the estimated resulting hip torque calculated from summation of these torques is sensitive to the precise values of these torques. Using inverse dynamics, the error of the calculated torques increases from ankle to knee to hip [31]. This hampers the determination of the FP. In the horizontal direction, the FP is displaced posteriorly relative to the CoM_{UB} (3 cm; figure 5). While the overall upper body oscillation is small (1.5° during single support [16], corresponding to a horizontal CoM_{UB} movement amplitude of less than 1 cm relative to the hip), the upper body rotates forwards during single support and backwards during double support. Because it starts rotating backwards at the end of the swing phase [16] as a result of leg retraction, we would expect positive resulting hip torques in the late stance phase. Hence, we would expect that the equivalent force should shift anteriorly in comparison with our estimate (figure 5*a*), causing the FP to shift anteriorly and inferiorly as well leading at the same time to a decreased quality of the FP. For more precise statements regarding the quality of the FP and more conclusive results regarding the FP location relative to the CoM_{UB}, a careful inverse dynamics calculation of individual hip torques and forces as well as a larger sample size are required. Nevertheless, we expect that the FP remains below the CoM_{UB}, which highlights the important contribution of other mechanisms in stabilizing the upper body such as postural reflexes at the hip [32,33].

In birds, the mechanical situation is very different from humans. Their heavy upper body is oriented horizontally and they have relatively lighter legs than humans [34]. The pronograde posture requires strong extension torques of the stance leg. Consequently, hip forces will be similar to GRFs and the hip torques of the stance leg will dominate the lever arm of the equivalent force. Thus, the FP will be above the CoM_{UB} and their upper body seems to be stabilized like a physical pendulum. These arguments point to a different approach in how the upper body is stabilized in humans versus birds or dinosaurs.

In upright walking, the fluctuations in the VPP model's [8] trunk (which contains the whole body mass) pitch angle were in phase with the whole body angle but opposite to the upper body angle of humans [14,18,19]. In contrast to the model's VPP, in human walking the FP is below the CoM_{UB} (figure 5*a*). Hence, the resulting torque acting on the upper body is in the opposite phase to that of the model and is consistent with the human upper body movement.

Maintaining a FP of net leg forces below the CoM_{UB} would lead to negative feedback when dealing with postural perturbations (figure 1*b*) that are introduced when tripping or unexpectedly stepping in a hole [21]. In contrast, maintaining a VPP above the CoM (in a coordinate frame that is rotationally fixed to the upper body) would be an appropriate reaction, because that would be associated with increasing the hip torques and restoring upper body posture, as was measured in [35]. Thus, we argue that the FP is not maintained during and after unexpected perturbations and therefore does not represent a control strategy. The FP's location is associated with resulting torques on the upper body of alternating sign, which is suitable for periodic movement, and with hip torques of low amplitude, a strategy that presumably reduces the metabolic cost of upright locomotion. Thus, it seems plausible that the FP location is a consequence of the tuning of the whole musculoskeletal system for efficient gait. Other mechanisms are required for upper body stabilization, e.g. hip reflexes or elastic muscle behaviour [36].

Ethics. All volunteers were physically active participants with no health problems that could have affected their performance or behaviour in this study. Informed written consent was obtained from each volunteer. The investigation was approved by the ethics review board of the University of Jena (3532-08/12) and was in accordance with the Declaration of Helsinki.

Data accessibility. Kinetic and kinematic data are deposited at https://doi.org/10.6084/m9.figshare.5478799.v1.

Authors' contributions. R.M., C.R. and R.B. developed the research question and designed the study. R.M., S.A. and J.V. performed the experiments and the data analyses. C.R. and R.M. interpreted the data and wrote the manuscript.

Competing interests. We declare we have no competing interests.

Funding. This research was partially supported by the German Research Foundation (DFG; MU 2970/4-1 to R.M.).

Acknowledgements. We thank Jens Schumacher (Institute of Stochastics, FSU Jena) for helping us with the statistical analysis and Kreg Gruben (University of Wisconsin - Madison) for the excellent and helpful review of the manuscript.

References

1. Crompton RH, Pataky TC, Savage R, D'Aout K, Bennett MR, Day MH, Bates K, Morse S, Sellers WI. 2012 Human-like external function of the foot, and fully upright gait, confirmed in the 3.66 million year old Laetoli hominin footprints by topographic statistics, experimental footprint-formation and computer simulation. *J. R. Soc. Interface* **9**, 707–719. (doi:10.1098/rsif.2011.0258)
2. Middleton KM, Gatesy SM. 2000 Theropod forelimb design and evolution. *Zool. J. Linn. Soc.* **128**, 149–187. (doi:10.1111/j.1096-3642.2000.tb00160.x)
3. Allen V, Bates KT, Li Z, Hutchinson JR. 2013 Linking the evolution of body shape and locomotor biomechanics in bird-line archosaurs. *Nature* **497**, 104–107. (doi:10.1038/nature12059)
4. Hutchinson JR, Allen V. 2009 The evolutionary continuum of limb function from early theropods to birds. *Naturwissenschaften* **96**, 423–448. (doi:10.1007/s00114-008-0488-3)
5. Geyer H, Seyfarth A, Blickhan R. 2006 Compliant leg behaviour explains basic dynamics of walking and running. *Proc. R. Soc. B* **273**, 2861–2867. (doi:10.1098/rspb.2006.3637)
6. Lipfert SW, Gunther M, Renjewski D, Grimmer S, Seyfarth A. 2012 A model-experiment comparison of system dynamics for human walking and running. *J. Theor. Biol.* **292**, 11–17. (doi:10.1016/j.jtbi.2011.09.021)
7. Andrada E, Nyakatura JA, Bergmann F, Blickhan R. 2013 Adjustments of global and local hindlimb properties during terrestrial locomotion of the common quail (Coturnix coturnix). *J. Exp. Biol.* **216**, 3906–3916. (doi:10.1242/jeb.085399)
8. Maus HM, Lipfert SW, Gross M, Rummel J, Seyfarth A. 2010 Upright human gait did not provide a major mechanical challenge for our ancestors. *Nat. Commun.* **1**, 70. (doi:10.1038/ncomms1073)
9. Andrada E, Rode C, Sutedja Y, Nyakatura JA, Blickhan R. 2014 Trunk orientation causes asymmetries in leg function in small bird terrestrial locomotion. *Proc. R. Soc. B* **281**, 20141405. (doi:10.1098/rspb.2014.1405)
10. Rummel J, Seyfarth A. 2010 Passive stabilization of the trunk in walking. In *Proceedings of SIMPAR 2010 Workshops: International Conference on Simulation, Modeling, and Programming for Autonomous Robots, Darmstadt, Germany, 15–16 November 2010*. Darmstadt, Germany: Technische Universität Darmstadt.
11. Sharbafi MA, Seyfarth A. 2015 FMCH: a new model for human-like postural control in walking. In *Proc. of the 2015 IEEE/RSJ Int. Conf. on Intelligent Robots and Systems* (*IROS*), *Hamburg, Germany, 28 September–2 October 2015*, pp. 5742–5747. New York, NY: IEEE.
12. Loeb GE, Brown IE, Cheng EJ. 1999 A hierarchical foundation for models of sensorimotor control. *Exp. Brain Res.* **126**, 1–18. (doi:10.1007/s002210050712)
13. Blickhan R, Andrada E, Müller R, Rode C, Ogihara N. 2015 Positioning the hip with respect to the COM: consequences for leg operation. *J. Theor. Biol.* **382**, 187–197. (doi:10.1016/j.jtbi.2015.06.036)
14. Gruben KG, Boehm WL. 2012 Force direction pattern stabilizes sagittal plane mechanics of human walking. *Hum. Movement Sci.* **31**, 649–659. (doi:10.1016/j.humov.2011.07.006)
15. Grasso R, Zago M, Lacquaniti F. 2000 Interactions between posture and locomotion: motor patterns in humans walking with bent posture versus erect posture. *J. Neurophysiol.* **83**, 288–300.
16. Aminiaghdam S, Rode C, Müller R, Blickhan R. 2017 Increasing trunk flexion transforms human leg function into that of birds despite different leg morphology. *J. Exp. Biol.* **220**, 478–486. (doi:10.1242/jeb.148312)

17. Saha D, Gard S, Fatone S. 2008 The effect of trunk flexion on able-bodied gait. *Gait Posture* **27**, 653–660. (doi:10.1016/j.gaitpost.2007.08.009)
18. Herr H, Popovic M. 2008 Angular momentum in human walking. *J. Exp. Biol.* **211**, 467–481. (doi:10.1242/jeb.008573)
19. Hirasaki E, Moore ST, Raphan T, Cohen B. 1999 Effects of walking velocity on vertical head and body movements during locomotion. *Exp. Brain Res.* **127**, 117–130. (doi:10.1007/s002210050781)
20. Müller R, Blickhan R. 2010 Running on uneven ground: leg adjustments to altered ground level. *Hum. Movement Sci.* **29**, 578–589. (doi:10.1016/j.humov.2010.04.007)
21. Müller R, Tschiesche K, Blickhan R. 2014 Kinetic and kinematic adjustments during perturbed walking across visible and camouflaged drops in ground level. *J. Biomech.* **47**, 2286–2291. (doi:10.1016/j.jbiomech.2014.04.041)
22. Gard SA, Miff SC, Kuo AD. 2004 Comparison of kinematic and kinetic methods for computing the vertical motion of the body center of mass during walking. *Hum. Movement Sci.* **22**, 597–610. (doi:10.1016/j.humov.2003.11.002)
23. Drillis R, Contini R, Bluestein M. 1964 Body segment parameters; a survey of measurement techniques. *Artif. Limbs* **8**, 44–66.
24. Zhao G, Seyfarth A. 2015 Contributions of stance and swing leg movements to human walking dynamics. In *Assistive robotics: Proceedings of the 18th International Conference on CLAWAR 2015* (eds H Su, T Wang, MO Tokhi, GS Virk), pp. 224–231. Singapore: World Scientific.
25. Aminiaghdam S, Rode C. 2017 Effects of altered sagittal trunk orientation on kinetic pattern in able-bodied walking on uneven ground. *Biol. Open* **6**, 1000–1007. (doi:10.1242/bio.025239)
26. Kluger D, Major MJ, Fatone S, Gard SA. 2014 The effect of trunk flexion on lower-limb kinetics of able-bodied gait. *Hum. Movement Sci.* **33**, 395–403. (doi:10.1016/j.humov.2013.12.006)
27. Bennett BC, Russell SD, Sheth P, Abel MF. 2010 Angular momentum of walking at different speeds. *Hum. Movement Sci.* **29**, 114–124. (doi:10.1016/j.humov.2009.07.011)
28. Silverman AK, Neptune RR, Sinitski EH, Wilken JM. 2014 Whole-body angular momentum during stair ascent and descent. *Gait Posture* **39**, 1109–1114. (doi:10.1016/j.gaitpost.2014.01.025)
29. Blickhan R. 1989 The spring-mass model for running and hopping. *J. Biomech.* **22**, 1217–1227. (doi:10.1016/0021-9290(89)90224-8)
30. Gruben KG, Boehm WL. 2014 Ankle torque control that shifts the center of pressure from heel to toe contributes non-zero sagittal plane angular momentum during human walking. *J. Biomech.* **47**, 1389–1394. (doi:10.1016/j.jbiomech.2014.01.034)
31. Winter DA, Patla AE, Frank JS. 1990 Assessment of balance control in humans. *Med. Prog. Through Technol.* **16**, 31–51.
32. Horak FB, Nashner LM. 1986 Central programming of postural movements: adaptation to altered support-surface configurations. *J. Neurophysiol.* **55**, 1369–1381.
33. Tang KS, Honegger F, Allum JH. 2012 Movement patterns underlying first trial responses in human balance corrections. *Neuroscience* **225**, 140–151. (doi:10.1016/j.neuroscience.2012.09.004)
34. Müller R, Birn-Jeffery AV, Blum Y. 2016 Human and avian running on uneven ground: a model-based comparison. *J. R. Soc. Interface* **13**, 20160529. (doi:10.1098/rsif.2016.0529)
35. Pijnappels M, Bobbert MF, van Dieen JH. 2005 How early reactions in the support limb contribute to balance recovery after tripping. *J. Biomech.* **38**, 627–634. (doi:10.1016/j.jbiomech.2004.03.029)
36. Tomalka A, Rode C, Schumacher J, Siebert T. 2017 The active force-length relationship is invisible during extensive eccentric contractions in skinned skeletal muscle fibres. *Proc. R. Soc. B* **284**, 20162497. (doi:10.1098/rspb.2016.2497)